

Single spike operation in SPARC SASE-FEL

M. Boscolo^{a,*}, M. Ferrario^a,
I. Boscolo^b, F. Castelli^b, S. Cialdi^b, V. Petrillo^b,
R. Bonifacio^c,
L. Palumbo^d
L. Serafini^e

^a INFN/LNF, Via Enrico Fermi 40, 00044 Frascati (Roma), Italy

^b University of Milano, Via Celoria 16, 20133 Milano, Italy

^c CBPF, Rio de Janeiro, Brazil

^d La Sapienza, Roma, Italy

^e INFN/MI, Via Celoria 16, 20133 Milano, Italy

Abstract

We describe in this paper a possible experiment with the existing SPARC photoinjector to test the generation of sub-picosecond high brightness electron bunches able to produce single spike radiation pulses at 500 nm in the SPARC self-amplified spontaneous emission free-electron laser (SASE-FEL). The main purpose of the experiment will be the production of short electron bunches as long as few SASE cooperation lengths and to validate scaling laws to foresee operation at shorter wavelength in the future operation with SPARX. The basic physics, the experimental parameters and 3-D simulations are discussed.

*Submitted to Special Issue of Nucl. Instrum. and Methods A for the International Workshop
'Frontiers in FEL Physics and related Topics, Elba Island, Italy, 8-14 September 2007*

* Corresponding author. Tel.: +39 06 94032636; fax: +39 06 94032256; e-mail: Manuela.Boscolo@Inf.infn.it.

1. Introduction

An electron bunch shorter than few cooperation length L_c can produce a short single radiation spike when injected in an properly tuned undulator via self-amplified spontaneous emission without any external seed, as proposed in ref [1,2]. The FEL regime of short electron and radiation pulses is called superradiant (SR). This regime has been studied in various theoretical and experimental works [3-9], with several debates upon its occurrence and features.

The superradiant regime requires the generation, acceleration and transport of high brightness short electron bunches, pushing the state of the art of existing photoinjectors to their extreme performances. In this paper we discuss the possibility to generate clean single radiation spikes with electron pulses produced by the existing SPARC photoinjector [10] equipped with a rf compressor [11], at wavelengths in the visible range (~ 500 nm).

In section 2 we present a scaling law useful for finding the suitable charge Q and bunch length L_b as a function of the FEL parameter ρ to fulfill the requirements of the single spike regime in the SASE operation. However, Q and L_b depend also on the temporal and transverse bunch shape. In section 3 and 4 we report a preliminary start to end simulation study of an optimized bunch in the SPARC linac able to produce a single radiation spike in a SASE-FEL. Beam dynamics simulations have been done with the code PARMELA [12] and the SASE-FEL radiation evolution has been calculated with the code GENESIS 1.3 [13].

2. Charge scaling law for single spike operation

A single radiation spike is generated in a SASE-FEL if the electron bunch length L_b satisfies the following condition [1,14]

$$L_b \leq 2\pi L_c = \frac{\lambda_r}{2\sqrt{3}} \frac{(1+\eta)}{\rho} \quad (1)$$

where L_c is the cooperation length

$$L_c = \frac{\lambda_r}{4\sqrt{3}\pi\rho} (1+\eta) \quad (2)$$

with λ_r the radiation length. The cooperation length is defined in the 1D FEL model as the slippage distance over one gain length. We have introduced in Eq. (1) the gain length degradation factor η introduced by M. Xie [14] in order to account for the additional 3D effects that all contribute to a degradation of the FEL performances: radiation diffraction, beam emittance and energy spread. The 1D FEL parameter ρ [15] is defined as

$$\rho = \left[\frac{1}{16} \frac{I}{I_A} \frac{K_o^2 [JJ]^2}{\gamma^3 \sigma_x^2 k_u^2} \right]^{1/3} \quad (3)$$

where $K_o = eB_o/(m_e c k_u)$ is the dimensionless wiggler parameter; $k_u = 2\pi/\lambda_u$ the undulator wavenumber, B_o the peak wiggler magnetic field; the Bessel factor $[JJ] = J_0(\xi) - J_1(\xi)$ is slightly below unity ($[JJ] = 0.85$) in our planar undulator case with $\xi = K_o^2 / (4 + 2K_o^2)$, $I_A \approx 17$ KA is the Alfvén current; I is the electron peak current and σ_x is the r.m.s. transverse size of the electron beam at the undulator entrance.

A convenient choice of bunch parameters can be done by using the scaling law derived by simple arguments in the following. Assuming condition (1) the average current I carried by the bunch can be written as:

$$I = \frac{Qc}{L_b} = \frac{2\sqrt{3}\rho Qc}{\lambda_r(1+\eta)} \quad (4)$$

This equation combined with Eq. (3) gives the scaling law for the bunch charge Q_{sp} that must be injected into the undulator in order to have a single FEL spike emission

$$Q_{sp} = \frac{8I_A k_u^2}{\sqrt{3c} K_o^2 [JJ]^2} \lambda_r \gamma^2 \varepsilon_n \beta_u (1+\eta) \rho^2 \quad (5)$$

where the r.m.s. bunch transverse size has been substituted by the relation $\sigma_x = \sqrt{\varepsilon \beta_u}$, β_u being the betatron length in the undulator, and the r.m.s. normalized emittance definition $\varepsilon_n = \gamma \varepsilon$ has been used.

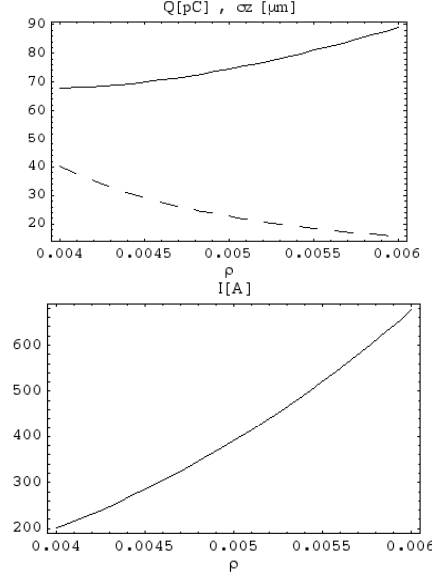


Fig. 1. Upper plot: bunch charge Q (pC) (full line) and size σ_z (μm) (dotted line) versus ρ ; lower plot: bunch current I versus ρ .

For example, with the SPARC FEL parameters reported in Table 1, Q_{sp} , σ_z and I behave as a function of ρ as shown in Fig. 1. Assuming a working point with $\rho = 5 \times 10^{-3}$ the optimal bunch charge results $Q \approx 75$ pC with a r.m.s. bunch length $\sigma_z \approx 25$ μm corresponding to a current of $I \approx 350$ A. It is worth mentioning that the Xie parameter for this case is $\eta = 1.1$, dominated by the radiation diffraction contribution and the resulting gain length is $L_g = 0.55$ m.

Table 1

SPARC FEL parameters.

λ_r (nm)	γ	$\Delta\gamma/\gamma$ (%)	ϵ_n (μm)	K_o	λ_u (cm)	β_u (m)
474	306	0.2	2	1.47	2.8	1.85

3. Electron beam generation

Such a high current electron beam cannot be generated directly by the gun because space charge effects produce a strong bunch elongation in the subsequent drift, as discussed in [16]. An additional compression mechanism is certainly required downstream the gun, that in the SPARC layout is performed by the first accelerating structure operating in the velocity bunching configuration [11].

We decided to start our optimization with a parametric beam dynamics study by scaling the nominal SPARC beam parameters ($Q=1$ nC, $\sigma_x=500$ μm and $\sigma_z= 860$ μm [17]) to the lower charge regime of interest for this application, according to the injector scaling law $\sigma_{x,y,z}(0) \propto Q^{1/3}$ [18], being $\sigma_{x,y,z}(0)$ the initial beam parameters at cathode.

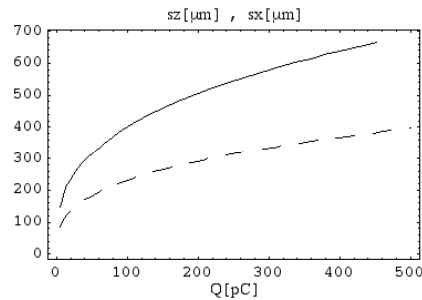


Fig. 2. Longitudinal and transverse beam size σ_z (μm) (full line) and σ_x (μm) (dotted line) as a function of the bunch charge Q .

As shown in Fig. 2 a 75 pC beam should have at the cathode $\sigma_x=220$ μm and $\sigma_z= 370$ μm to preserve the emittance compensation optimization of the nominal case. To properly match this beam to the undulator a

compression factor higher than 10 is required, together with a spot size demagnification down to $\sigma_x = \sqrt{\epsilon\beta_u} = 110 \mu\text{m}$, see Table 1.

We have performed PARMELA simulations with different bunch charges, ranging from 25 to 500 pC. The summary of the resulting parameters at the entrance of the undulator are listed in Table 2 where the last row gives the correspondent peak radiation power, discussed in more details in section 4.

Table 2

Summary of the electron beam and radiation parameters obtained for different bunch charge.

Q (pC)	25	50	100	300	500
$\sigma_z(\mu\text{m})$	19	23	28	64	71
$\sigma_x(\mu\text{m})$	97	129	173	227	253
$\epsilon_{x,rms}(\mu\text{m})$	1.49	2.32	3.36	8.18	10.12
I (A)	160	260	420	560	840
$\Delta E/E$ (%)	0.206	0.229	0.220	0.443	0.533
$\rho(10^{-3})$	4.11	3.99	3.84	3.32	3.73
η	2.29	2.0	1.42	7.49	8.6
$L_{g3d}(\text{m})$	1.02	1.0	0.81	3.0	3.3
$L_c(\mu\text{m})$	7.5	8.5	6.9	26.4	28.5
$L_b/2\pi L_c$	0.85	1.07	1.6	0.96	0.98
P(MW)	9.25	105	640	1370	1900

3.1 50 and 100 pC electron bunches evolutions

The evolution of the beam envelope and emittance during emittance compensation and velocity bunching sections up to the end of the accelerator are shown in plot of Fig. 3 for the compressed and uncompressed 50 pC bunch case.

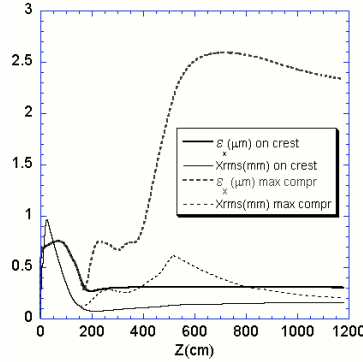


Fig. 3. Beam emittance and envelope at maximum compression (dotted line) compared to uncompressed case (full line), for a 50 pC bunch.

The 100 pC case has a similar behaviour to the 50 pC one, except for a larger final emittance of 3.4 μm instead of 2.3 μm .

The optimized phase for maximum compression results to be -91.4° and -91° for the 50 and 100 pC, respectively. Beam current profiles for the 50 and 100 pC bunch charge case at the end of accelerating sections are shown in Fig. 4.

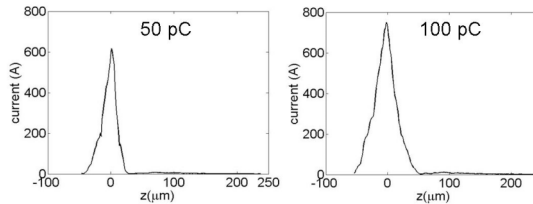


Fig. 4. Left and right frames: beam current profile of 50 pC and 100 pC bunch charge, respectively.

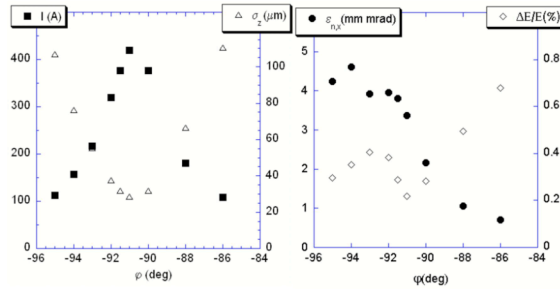


Fig. 5. Left Frame shows average current and bunch length, right frame shows emittance and energy spread as a function of the RF compressor injection phase for a 100 pC bunch charge case.

Fig. 5 shows the dependence of peak current, emittance and energy spread on RF phase: the more compressed is the bunch the worse is the emittance.

Fig. 6 shows the variation of the pulse shape (current and length) due to a 1° shift of the RF compressor injection phase. The pulses, even having much different current profiles, still fulfill the condition for single spike generation, as we have checked with GENESIS simulations. We note the phase jitter in our accelerator is less than 1° . The sensitivity to phase jitter is reduced of a factor greater than two by the use of the IV harmonic section [19].

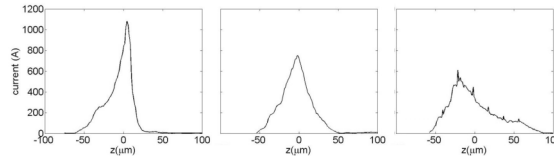


Fig. 6. Plots from left refer to beam current profile respectively for injection phase of -92° , -91° and -90° , at the end of linac for a 100pC pulse.

4. SASE FEL Simulations

Electron pulses given by PARMELA simulation code (whose parameters are listed in Table 1) has been transported into the undulator and FEL interaction has been simulated with GENESIS 1.3 code [13]. Focusing quadrupoles inside the undulator have not yet been included in these studies. We have performed start-to-end simulations for pulses of 25, 50, 100, 300 and 500 pC bunch charge. The irregular shape of the current profiles summed to a notable transverse dimension variation along electron bunches leads to a FEL parameter ρ variable along the pulse (in fact, each slice of the beam experiences a different gain). Because of this we introduce an average value of the ρ parameter and refer to that value for the quotation of the cooperation length. With the ρ parameter values listed in Table 2 the cooperation length turns out in between 7 and 28 μm . The output radiation pulses obtained with the set of electron bunches are shown in Fig. 7: all plots show a single radiation spike, as expected. They, except for the 25 pC case, are plotted at the point z_{max} , where the peak of the radiation pulse overcomes the electron bunch, reaching its maximum value. The 25 pC charge case (first from top) is plotted at the end of the undulator because the corresponding z_{max} is longer in this case than the 14 m SPARC undulator. This fact makes the first case different from the others. The higher is the charge, the shorter results z_{max} and the higher is the peak power.

The cleaning of both pulse and spectrum (which are wider and spiky at the start-up from shot noise) occurs at an early stage of the emission process. In the very first stage, the radiation comes only from the regions of larger current. When the tail slices with larger radius and lower current begin to radiate, there is a slight enlargement of the radiation pulse, followed by a successive narrowing.

The temporal width of the radiation pulses squeezes towards higher current (plots from top to bottom in Fig. 7) and reach a length of around 70 fs. The spectrum of the three central pulses evolves shifting the central frequency and peaking it enormously. We have noticed a fast phase variation in the output phase diagrams. It is interesting to note that the 500 pC bunch still provides a clean single spike (at $z_{\text{max}}=9$ m) but its spectrum profile is much spiky. The narrowest spectrum relative to the 25 pC electron bunch complies with the largest pulse profile because a clear phase chirp is present in its FEL simulations.

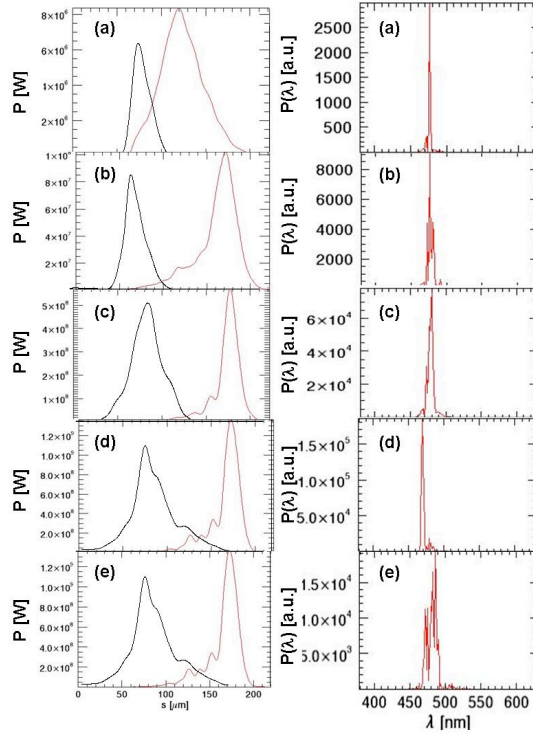


Fig. 7: Columns from left show, respectively, the power profile along the bunch coordinate $s(\mu\text{m})$ (in red) and superimposed in black the current profile and radiation spectrum at z_{max} . Rows from top are: (a) 25 pC, $z_{\text{max}} = 13$ m, (b) 50 pC, $z_{\text{max}} = 12$ m, (c) 100 pC, $z_{\text{max}} = 11$ m, (d) 300 pC, $z_{\text{max}} = 10$ m, (e) 500 pC, $z_{\text{max}} = 9$ m.

The dependence of the power P on the bunch charge Q is reported in Fig. 8, where $\log P$ is shown versus $\log(Q^2)$. The straight line fitting (approximately) the first three points has angular coefficient of 1 (in red) whereas the second one has an angular coefficient of $2/3$. We observe that for the first points the peak power scales like Q^2 as predicted by the SR theory [1], while the other points scale like $Q^{4/3}$ as by the standard SASE-FEL theory.

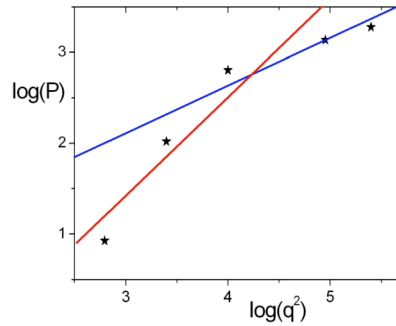


Fig. 8. Markers show simulations results of peak power P as a function of the bunch charge squared Q^2 in a logarithmic scale; the red line is: $\log P = \log Q^2 + \text{const}$; the blue line is $\log P = 2/3 \log Q^2 + \text{const}$.

From the lines' slopes we may say that, in correspondence to $Q=100$ pC, a transition between two different regimes occurs. In this connection we stress that the characteristics (ϵ , ΔE , L_b , I and σ_x) of the electron bunches with different charge at the output of the accelerator are notably different, this leads to a different SASE-FEL operation on each of them. In particular, the two cases with higher current are strongly dominated by the energy spread, whereas the first three cases are dominated by diffraction effects. The extraction of a general conclusion from the $P=f(Q)$ diagram is, therefore, matter of discussion.

In the present work the scaling law has been useful as a starting point for our simulations. A more systematic study with the scaling law is underway with an ideal beam.

The following other observations are worth:

1. The spiky behavior of the spectrum relative to the 500 pC charge bunch indicates that charge as the limit for a clean single spike generation.
2. The regime of single spike radiation is also affected by strong shot to shot fluctuations on the radiation growth length and on the peak power value.

3. Since a single radiation spike, together with the output electron bunch, can be fully analyzed with the today optical and electromagnetic diagnostic tools, we have the possibility to investigate the SR regime in the SPARC setup.

4. Conclusions

Preliminary start to end simulations of a possible experiment with the existing SPARC setup to test the generation of sub-picosecond high brightness electron bunches able to produce single spike radiation pulses at 500 nm have been discussed.

Investigation of a low charge regime is required for this kind of experiment as predicted by the charge scaling laws derived in this paper. Future experiments with the 2 GeV SPARX linac designed to drive FEL single spike at 3 nm discussed in [20] will require even lower charge, see Fig. 9, hence a preliminary test at 500 nm will be a very good training experiment.

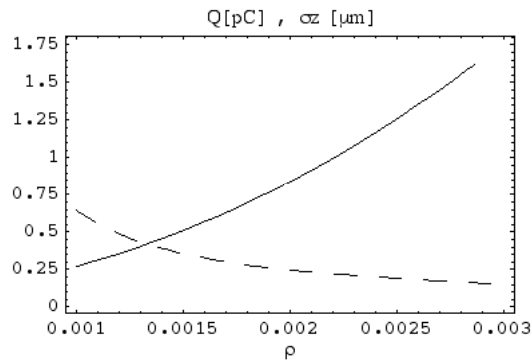


Fig. 9. Bunch charge Q (pC) (full line) and size σ_x (μm) (dotted line) versus ρ for the 2 GeV SPARX case [19].

Further studies to implement the production of clean radiation spikes by a comb electron beam properly tuned are also in progress [21].

Acknowledgements

This work has been partially supported by the EU Commission in the sixth framework program, contract n. 011935 EUROFEL and n.RII3-CT-PHI506395CARE.

References

- [1] R. Bonifacio et al. PRL 73 (1994) 70.
- [2] R. Bonifacio et al., Int J Infrared Milli Waves (2007) 28: 699-704
- [3] R. Bonifacio, F. Casagrande NIMA 239 (1985) 36.
- [4] R. Bonifacio and B.W.J. McNeil NIMA 272 (1988) 280.
- [5] R. Bonifacio, B.W.J. McNeil, P.Pierini PRA 40 (1989) 4467.
- [6] R. Bonifacio et al. NIMA 296 (1990) 358.
- [7] D. A. Jaroszynski et al. PRL 78 (1997) 1699.
- [8] N. Piovella: Phys of Plasmas 6(1999) 3358.
- [9] T. Watanabe, X.J. Wang, J.B. Murphy et al. PRL 98 (2007) 034802.
- [10] Alesini et al. in PAC Proceedings, Albuquerque, NM, 2007 p.80.
- [11] L. Serafini and M. Ferrario, "Velocity Bunching In Photo-Injectors", Proc. of 20th ICFA Beam Dynamics Workshop on "Physics of, and Science with, the X-ray Free-Electron Laser" Arcidosso (Italy), Settembre 10-15, 2000
- [12] J. Billen, PARMELA, LA-UR-96-1835, 1996.
- [13] S. Reiche: Genesis 1.3. Nucl. Instrum. Methods Phys. Res. A 429, 243 (1999), <http://pbpl.physics.ucla.edu/~reiche/>
- [14] M. Xie, in Proceedings of the 1995 Particle Accelerator Conference (IEEE, Piscataway, NJ, 1995), p. 183.
- [15] R. Bonifacio, C. Pellegrini and L. Narducci, Opt. Comm. 50 (1984) 313.
- [16] L. Serafini, AIP Conf. Proc. 413 (1997) 321.
- [17] M. Ferrario et al., SLAC-PUB-8400 (2000).
- [18] J.B. Rosenzweig, N. Barov and E. Colby, IEEE Trans. Plasma Sci. 24, 409 (1996).
- [19] C. Ronsivalle et al, in Proceedings of the 2005 Particle Accelerator Conference (IEEE, Knoxville, TN, 2005) p. 1144.
- [20] J.B. Rosenzweig et al, These Proceedings
- [21] M. Boscolo, I. Boscolo, F. Castelli, S. Cialdi, M. Ferrario, V. Petrillo and C. Vaccarezza, These Proceedings.